

Original Article

Corrosion of neutron/gamma-irradiated aluminium alloy 6061

Kotchaphan Kanjana* and Jatechan Channuie

*Division of Research and Development, Thailand Institute of Nuclear Technology,
Ongkharak, Nakhon Nayok, 26120 Thailand*

Received: 7 May 2017; Revised: 1 December 2017; Accepted: 6 October 2017

Abstract

Effect of mixed neutron/gamma radiation on corrosion of aluminum alloy 6061 (AA6061) was studied. Square-shaped AA6061 samples were exposed to mixed neutron/gamma radiation continuously in the Thai Research Reactor-1/Modification 1 (TRR-1/M1), and gamma radiation from the Co-60 radiation source at the Gems Irradiation Center, Thailand Institute of Nuclear Technology (TINT). Dose-effect of the mixed radiation was investigated at neutron fluence and gamma ray of $1.7\text{-}3.9 \times 10^{18}$ n/cm² and 218 kGy, respectively. For comparison, separate effect of gamma radiation on corrosion of AA6061 was also examined at the total dose up to 600 kGy. Characterization using SEM-EDX revealed that AA6061 exposed to the mixed radiation resulted in the development of amorphous-like corrosion products with no pitting corrosion observed, whereas exposing to gamma radiation assisted in pitting corrosion through the formation of crystal-like corrosion products (bayerite and boehmite).

Keywords: corrosion, aluminum alloy, research reactor, neutron/gamma radiation, SEM-EDX

1. Introduction

Ionizing radiations produced in a nuclear research reactor (neutron, gamma and beta) can potentially induce corrosion in materials, especially aluminum alloy 6061 (AA6061), the most widely used structural material in research reactors. Irradiation-induced corrosion in metal alloys has been found to originate from the combination of direct and indirect effects. The direct effect results from the direct interactions between the radiation (gamma, neutrons, electrons or ions) and the alloys which may lead to changes in microstructure, microchemistry and composition of the alloys (Bruemmer & Was, 1994). The indirect effect stems from the electrochemical reactions between the radiolytic primary species ($e^-_{(aq)}$, $\cdot\text{OH}$, $\cdot\text{H}$, H_2 , H_2O_2 and HO_2/O_2^-) generated in water coolant and the atoms on the alloy surfaces (Cuba, Mucka, & Pospisil, 2012; Lin, Kim, Niedrach, & Ramp, 1996; Scott, 1994). The combination of irradiation-induced corrosion and other factors, such as stress and strain within the material,

temperature and pressure of the system, can cause peeling of the unstable outer oxide layer on the material surface. In time this cycling process, so-called Irradiation-Assisted Stress Corrosion Cracking (IASCC), can ultimately bring about material cracking (Kritzler, 2004; Lin, 2009; Scott, 1994).

As of now, the available information regarding irradiation-induced corrosion of AA is very limited. Oxide formation as well as time and radiation dose effects were completely ignored in the previous studies (IAEA, 2003; Kumar, Baheti, & Chacharkar, 1989). According to the literature, it can be clearly seen that the following information are still missing: 1) The effect of mixed neutron/gamma radiation on AA; 2) Dose-effect of mixed neutron/gamma on AA at the dose levels comparable to those in research reactors; 3) Chemical structure of the oxide generated on AA surface under the operational conditions of research reactors.

The present research aimed to investigate the effect of ionizing radiations on corrosion of AA in a broader scope to cover all missing aspects from the literature and to obtain necessary information for handling corrosion problem of AA in research reactors. The effect of mixed neutron/gamma radiation with varied radiation dose was studied using Thai Research Reactor-1/ Modification 1 (TRR-1/M1) as radiation source. The separate effect of gamma radiation generated from a Co-60 radiation source was also studied. The chemical

*Corresponding author

Email address: kotchaphank@tint.or.th,
kotkanjana@gmail.com

structures of the oxides produced on the sample surface were examined to gain insight into the corrosion level and corrosion type.

2. Experimental Section

2.1 Sample preparation

The AA 6061 samples (dimensions of 2 cm x 2 cm x 0.2 cm) from Southwest Aluminum (Group) Co., LTD were wet polished using a Buehler MetaServ 250 Twin polisher with abrasive grinding paper (grit sizes ranging from 360 grit to 1,200 grit). To remove polishing and organic residues, the samples were subsequently ultrasonic cleaned with organic solvents including acetone, methanol and ethanol. The samples were then left to dry in air and kept in a desiccator at room temperature before weighing. Finally, the chemical composition of the unirradiated samples was analyzed using an X-ray Fluorescence (XRF) spectrometer (Bruker, S8 TIGER).

2.2 Sample irradiation

For mixed neutron/gamma irradiation, the AA6061 samples were allowed to expose to the radiation in the load tubes of TRR-1/M1 at different levels of radiation flux. Gamma irradiation was performed using a Co-60 source (30366 Ci) with varied irradiation times. In both experiments, the alloy samples were fully immersed in demineralized water (pH 5.6 with the conductivity of 2 μ S/cm and dissolved oxygen concentration of 9.03 mg/L). The temperatures during irradiation in both cases were about 33 °C. The neutron flux in the irradiation tubes of TRR-1/M1 was measured using neutron flux monitors. The flux was later converted into fluence. For gamma dosimetry, Harwell Amber Perspex dosimeter which was cast sheets of poly-methylmethacrylate (PMMA) was used throughout the experiments. This dosimeter provided +/- 1% of uniformity in a radiation field.

2.3 Post-irradiation characterization

After irradiation, the alloy samples were air-dried, and the activated elements within the samples were allowed to decay completely before characterization. The radioactive decay measurement of gamma-ray photons was made by a gamma spectrometer with 60% relative efficiency of high purity germanium and a resolution of 1.9 keV at 1.33 MeV (ORTEC Industries). Eventually, the oxide morphology on the sample surface and its composition profile were analyzed using Scanning Electron Microscopy–Energy Dispersive X-Ray Spectroscopy (SEM-EDX, JEOL JSM-5410).

3. Results and Discussion

3.1 Unirradiated AA6061

To ensure the aluminum alloy received from the manufacturer was AA6061, the chemical composition of the unirradiated samples was examined using XRF. Table 1 shows the chemical compositions of the samples from XRF analysis and the manufacturer certificate in comparison with that of AA6061 standard (Designation-B209-04, 2005). It can be seen that within the detection error the chemical composition of the alloy received falls in the range of the manufacturer and the standard values.

The surface morphology of the blank sample was also investigated using SEM-EDX technique. As shown in Figure 1, all over the sample surface was found to be non-uniform with two distinct features. One was expectedly smooth surface mainly composed of Al (Spectrum 2) and the other was darker areas (Spectrum 1) containing Si and Mg in addition to Al. Si and Mg are known to be added during alloy precipitation for strengthening purpose. The carbon component detected was a contaminant from the sample preparation process.

3.2 Mixed neutron/gamma-irradiated AA6061

Mixed neutron/gamma irradiation was successfully done in TRR-1/M1 A4 and CA2 load tubes with neutron fluence and gamma dose in the ranges of $1.7\text{-}3.9 \times 10^{18}$ n/cm² and 218 kGy, respectively. It is known that interactions between neutrons and alloys can cause phenomena, such as defects in the crystal structure, changes in mechanical properties and physical dimensions of the materials. Neutron radiation damage is generally measured in the unit of displacements per atom (DPA). Based on a previous study (Ampornrat, Boonsuwan, Sangkaew, & Angwongtrakool, 2017), DPA in TRR-1/M1 of AA6061 caused by fast neutrons was found to be 4 dpa. However, it should be noted that the present study aimed to investigate the effect of neutron on AA6061 corrosion in general. Therefore, separate effects of neutron at different energies (thermal, epithermal and fast neutrons) will not be part of the discussion.

The morphology of the AA6061 samples exposed to mixed neutron/gamma radiation is illustrated in Figure 2. It can be clearly seen in Figure 2a that after exposing to low fluence (1.7×10^{18} n/cm²) there is no evidence of corrosion product on the sample surface. However, it appears to have crack-like features on the surface of the samples which was not found in the samples exposed to high fluence (3.9×10^{18} n/cm²) (see Figure 2b). These non-corresponding results indicate that the phenomenon may not be relevant to irradiation.

Table 1. Chemical composition of the unirradiated AA6061 samples examined by XRF and the one indicated in the manufacturer certificate in comparison with that of AA6061 standard (Designation-B209-04, 2005).

Element	Si	Fe	Cu	Mn	Mg	Cr	Zn	Ti	Al	% error
AA6061 Standard	0.40-0.80	≤ 0.70	0.15-0.40	≤ 0.15	0.8-1.2	0.04-0.35	≤ 0.25	≤ 0.15	Remainder	-
Certificate	0.74	0.20	0.27	0.04	0.90	0.14	0.03	0.02	97.66	-
XRF	0.86	0.26	0.26	-	0.84	0.16	0.07	-	97.32	0.5

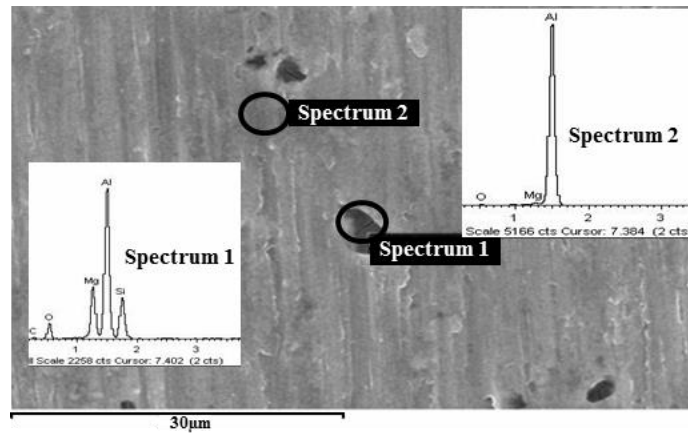


Figure 1. Surface morphology of the blank AA6061 sample taken by SEM-EDAX.

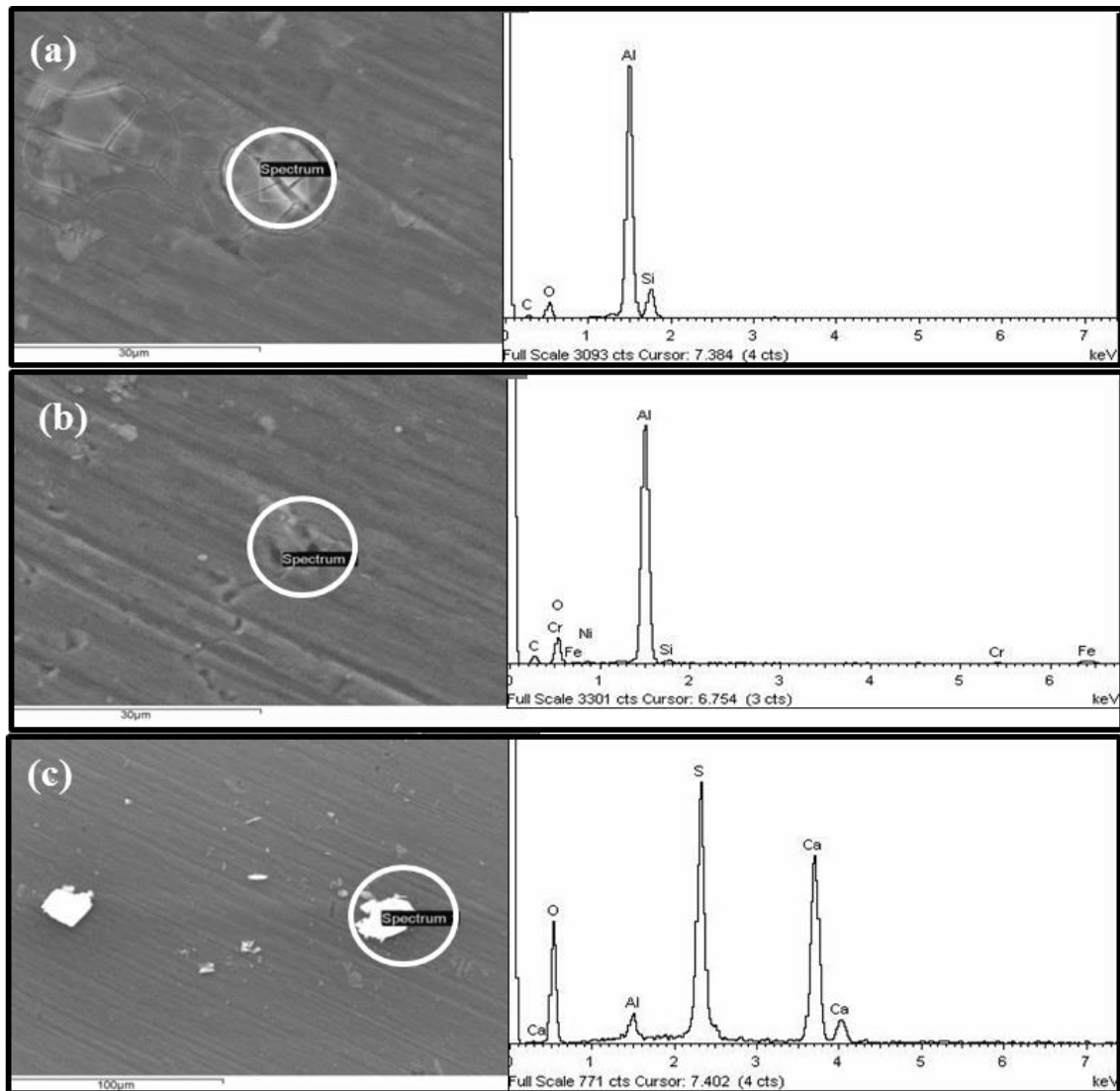


Figure 2. Surface morphology of AA6061 samples exposed to mixed neutron/gamma (26 hrs): (a) exposed to 1.7×10^{18} n/cm², (b) exposed to 3.9×10^{18} n/cm² and (c) corrosion product after exposing to 3.9×10^{18} n/cm².

This challenging issue is left for our future investigation. In addition, the evidence of corrosion products was found in the sample exposed to higher neutron fluence (Figure 2c.) The corrosion products observed contains O, S and Ca in addition to Al matrix element. The O component implicates oxide formation on the sample surface. At room temperature the corrosion products generated from oxidation of Al in water are commonly found in the form of amorphous alumina (Vargel, 2004; IAEA, 2003) or a crystalline aluminum hydroxide AlO(OH), boehmite (Farrell, 2012). With continued immersion in water, the latter product may eventually transform in to a crystalline aluminum hydroxide (Al(OH)₃), so-called bayerite. However, considering our experimental conditions (temperature and pH) in conjunction with the features of the corrosion products virtually observed in Figure 2c, the products in this experiment are presumably amorphous alumina. The traces of S and Ca detected were likely to come from demineralized water.

3.3 Gamma-irradiated AA6061

In order to study separate effect from gamma radiation, AA6061 samples were irradiated with gamma radiation for 100 hrs (300 kGy) and 200 hrs (600 kGy) while immersing in demineralized water. The sample morphology from the gamma experiments taken by a confocal microscope can be seen in Figure 3. After immersing in demineralized water for 100 hrs without exposing to radiation, some brown spots were observed on the sample surface (Figure 3a). When the sample was allowed to expose to 300 kGy of gamma radiation, a number of dark spots were detected (Figure 3b.). The dark spots seem to develop from the brown spots shown in Figure 3a. It was reported previously pitting corrosion is the major corrosion type found in AA in contact with water (Davis, 1999; Farrell, 2012; Zaid, Saidi, Benzaid, & Hadji, 2008). Therefore, it is reasonable to believe that with higher gamma radiation dose, the dark spots will evolve into pitting corrosion. To verify this assumption, 600 kGy of gamma radiation was used to perform an additional experiment, the results of which are demonstrated in Figure 3d. Unfortunately, the morphology taken by the confocal microscope did not give a good comparison between the results from the control (Figure 3c.) and the experimental (Figure 3d.) sets. Therefore, the sample exposed to 600 kGy of gamma radiation and the control set were later characterized by SEM-EDX as shown in Figure 4. The SEM micrographs shown in Figures 4a and 4b clearly show the effect of gamma radiation on pitting corrosion of the AA6061 sample. More pits were developed in the sample exposed to 600 kGy of gamma radiation compared to the controlled sample in Figure 4a. It is implicit that with higher gamma dose the sample surface is more corroded producing corrosion products with higher density. The EDX spectra of the corrosion products appearing around and on the pits can be seen in Figures 5a and 5b. The results reveal that the %wt ratios of Al:O of the products around and on the pits are approximately 64:36 and 53:47 indicating the formation of bayerite (Al(OH)₃) and boehmite (AlO(OH)), respectively. Both aluminum hydroxides have been proven to stabilize in the crystal structure (Farrell, 2012).

As mentioned previously neutron irradiation can have direct effects on alloying materials by changing their crystal structures, mechanical properties and physical

dimensions. The subsequent corrosion process of the materials can be inevitably determined by these phenomena. It was expected that for the samples exposed to mixed neutron/gamma radiation the direct effects of neutron irradiation on the material would dominate the corrosion process of the samples. The results from the present work clearly show that under the experimental conditions the main difference between the samples exposed to mixed neutron/gamma and gamma radiations are the developments of corrosion type and products. Pitting corrosion was unobservable in the mixed neutron/gamma irradiated samples, whereas this type of corrosion was obviously seen in the gamma irradiated surface. In addition, the corrosion product found in the former case seems to be amorphous alumina. In the latter case, however, the corrosion products are proven to be crystal aluminum oxides (bayerite and boehmite).

4. Conclusions

Effects of mixed neutron/gamma and gamma radiations on corrosion of AA6061 were investigated. The post-mixed neutron/gamma irradiated AA6061 appeared to have a corrosion product (amorphous aluminum hydroxide) with higher flux. Gamma radiation exposure assisted in pitting corrosion through the formation of crystalline aluminum hydroxides with higher density compared to that of the mixed neutron/gamma irradiation study.

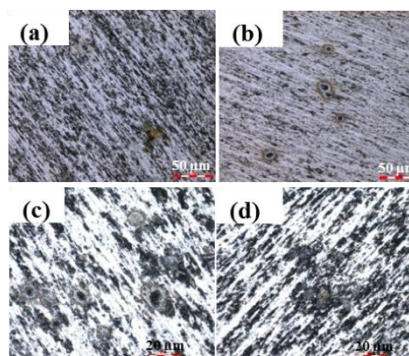


Figure 3. Surface morphology of AA6061 samples from gamma radiation experiments taken by a confocal microscope: (a) 100 hrs of immersion in demineralized water without exposing to gamma radiation, (b) 100 hrs of immersion in demineralized water while exposing to 300 kGy of gamma radiation, (c) 200 hrs of immersion in demineralized water without exposing to gamma radiation and (d) 200 hrs of immersion in demineralized water while exposing to 600 kGy of gamma radiation.

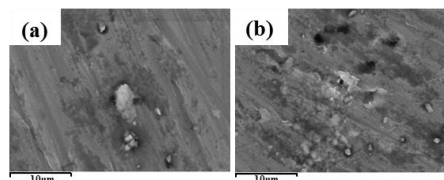


Figure 4. Surface morphology of AA6061 samples from gamma radiation experiments taken by SEM: (a) 200 hrs of immersion in demineralized water without exposing to gamma radiation, (b) 200 hrs of immersion in demineralized water while exposing to 600 kGy of gamma radiation.

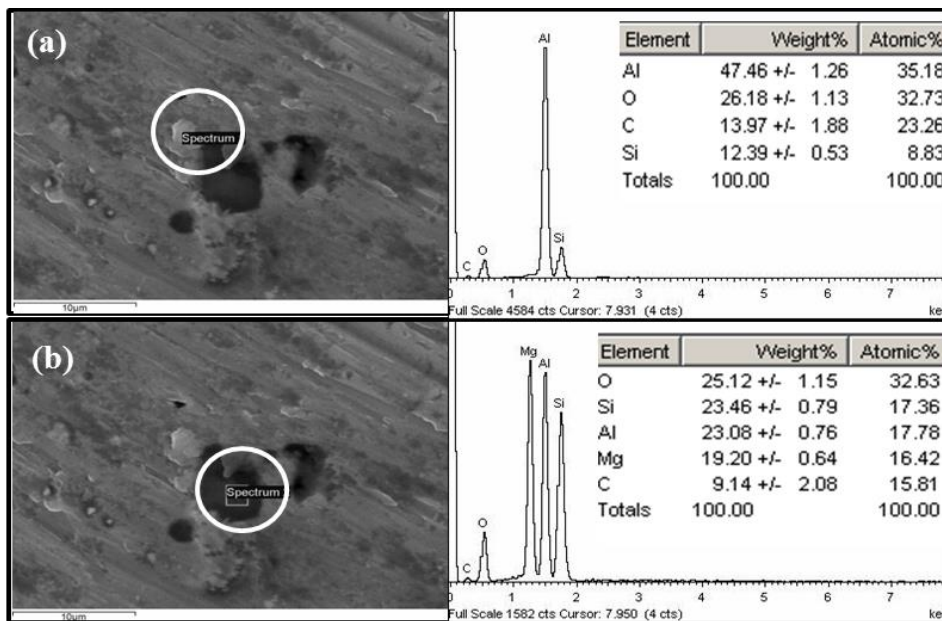


Figure 5. Surface morphology of AA6061 samples after 200 hrs of immersion in demineralized water while exposing to 600 kGy of gamma radiation taken by SEM: (a) with EDX spectrum of the corrosion product around the pit (b) with EDX spectrum of the corrosion product covering the pit.

Acknowledgements

The research herein was supported by the Coordinating Center for Thai Government Science and the Technology Scholarship Students (CSTS) and the National Science and Technology Development Agency (NSTDA). The authors are also grateful to Ms S. Ouampan at the Failure Analysis and Materials Degradation (FAMD) Unit, National Metal and Materials Technology Center (MTEC).

References

- Ampornrat, P., Boonsuwan, P., Sangkaew, S., & Angwongtrakool, T. (2017). Preliminary study of degradation from neutron effects of core-structural materials of Thai Research Reactor TRR-1/M1. *Journal of Physics: Conference Series*, doi:10.1088/1742-6596/860/1/012042
- Bruemmer, S. M., & Was, G. S. (1994). Effects of irradiation on intergranular stress corrosion cracking. *Journal of Nuclear Materials*, 216, 326-347.
- Cuba, V., Mucka, V., & Pospisil, M. (2012). Radiation induced corrosion of nuclear fuel and materials. In S. T. Revankar (Ed.), *Advances in nuclear fuel* (pp. 27-52). Vienna, Austria: InTech.
- Davis, J. R. (1999). *Corrosion of aluminum and aluminum alloys*. Materials Park, OH: ASM International.
- Designation-B209-04. (2005). *Standard specification for aluminum and aluminum-alloy sheet and plate*. West Conshohocken, PA: ASTM international.
- Farrell, K. (2012). Performance of aluminum in research reactors. In R. J. M. Konings (Ed.), *Comprehensive nuclear materials: vol. 5.07* (pp. 143-175). Waltham, MA: Elsevier.
- International Atomic Energy Agency. (2003). *Technical reports series 418: Corrosion of research reactor aluminium clad spent fuel in water* (IAEA Library Cataloguing in Publication Data). Vienna, Austria.
- Kritzer, P. (2004). Corrosion in high-temperature and supercritical water and aqueous solutions: A review. *Journal of Supercritical Fluids*, 29, 1-29.
- Kumar, R., Baheti, G. L., & Chacharkar, M. P. (1989). Corrosion behaviour of aluminium in the presence of neutrons and gamma radiations. *Journal of Radio-analytical and Nuclear Chemistry*, 132, 3-9.
- Lin, C. C. (2009). A review of corrosion product transport and radiation field buildup in boiling water reactors. *Progress in Nuclear Energy*, 51, 207-224.
- Lin, C. C., Kim, Y. J., Niedrach, L. W. & Ramp, K. S. (1996). Electrochemical corrosion potential models for boiling-water reactor applications. *Corrosion*, 52, 618-625.
- Scott, P. A. (1994). Review of irradiation assisted stress corrosion cracking. *Journal of Nuclear Materials*, 211, 101-122.
- Vargel, C. (2004). *Corrosion of aluminium*. New York, NY: Elsevier.
- Zaid, B., Saidi, D., Benzaid, A., & Hadji, S. (2008). Effects of pH and chloride concentration on pitting corrosion of AA6061 aluminum alloy. *Corrosion Science*, 50(7), 1841-1847.